International Journal of Mechanical and Production
Engineering Research and Development (IJMPERD)
ISSN(P): 2249-6890; ISSN(E): 2249-8001
Vol. 3, Issue 5, Dec 2013, 165-172

CFD BASED ANALYSIS OF HEAT TRANSFER AND FRICTION CHARACTERISTICS OF BROKEN MULTIPLE RIB ROUGHENED SOLAR AIR HEATER DUCT

RAJ KUMAR, VISWAMOHANPEDAGOPU, ANIL KUMAR, ROBIN THAKUR & ANIL PUNDIR

Mechanical Engineering Department, Shoolini University, Solan, Himachal Pradesh, India

ABSTRACT

This paper presents the results of aCFD based analysis on heat transfer and friction characteristics to the air flow in the rectangular duct. The upper side of heated plate is made rough with circular ribs of broken multi v-rib. The results of the broken multi v-rib the significant increase in heat transfer rate and friction loss over the smooth surface. The relative gap width (g/e) 1.0 rib provided the highest broken multi v-riband CFD model results were compared with broken multi v-rib, Realizable k-epsilon model results have been found to have good agreement.

KEYWORDS: Renewable Energy, Heat Transfer, Broken Rib

INTRODUCTION

Improvement in the thermo hydraulic performance of a solar air heater can be done by enhancing the heat transfer. In general, heat transfer enhancement techniques are divided into two groups: active andpassive techniques. Providing an artificial roughnesson a heat transferring surface is an effective passiveheat transfer technique to enhance the rate of heattransfer to fluid flow. Beside a relative roughness height and angle of attack, shapes of various roughness elements also influence the heat transfer rate and friction factor investigated a various investigators details are given below:

The Stanton number for V-down discrete ribs was higher than the corresponding V-up and transverse discrete roughened surfaces [1, 2]. Karwa [3] has investigated and revealed the effect of transverse, inclined, V-continuous and V-discrete patterns on heat transfer and the frictionfactor in a rectangular duct.

Broken V-shaped or broken parallel ribs can create more secondary flow cells and produce more local turbulence in the opposite wall region in comparison to the continuous V-shaped or continuous parallel ribs. The average heat transfer coefficient for the ribbed surfaces turned out to be higher thanthose for the ribbed surface by a factor of up to 2 when the transverse ribs were continuous, and by a factor of up to 3 when they were broken.

Sahu and Bhagoria [4] investigatedexperimentally the effect of pitch varying from10 to 30 by taking the height of the rib to be1.5 mmand duct aspect ratio 8 on the heat transfer coefficientand friction factor for 90° broken transverseribs. It was found that the separation occurred notonly at the top edge of the rib but also at the edgesat the end of the ribs. This secondary flow interruptedthe growth of the boundary layer downstreamof the nearby attachment zone in case of90° broken ribs.

Aharwalet al. [5, 6] investigated the effect of gap to width ratio (g/e) andgap to position ratio (d / W) in an inclined split ribarrangement in a rectangular duct of a solar airheater.

Saini and Verma [7] investigated the effect ofrelative roughness height (e/D) and relative roughnesspitch (P/e) of dimple-shape roughness geometryon heat transfer and friction factor.

Bopche and Tandale [8] investigated experimentallythe effect of the inverted U-shaped turbulatorson the absorber surface of an air heater ducton the heat transfer coefficient and friction factor.

COMPUTATIONAL FLUID DYNAMICS

Computational fluid dynamics is analysis of the system involving fluid flow, heat transfer and associated phenomena such as chemical reaction by means computer based simulation.

In this investigation a three-dimensional numerical simulation of the heat transfer and friction factor was conducted using the Computational fluid dynamics (GAMBIT and FLUENT) software.The modeling carried out in order to predict and explain the experimental observations.The CFD modeling involves numerical solutions of the conservation equations for mass, momentum and energy.These equations for incompressible flows can be written as follows:

Mass Conservation

$$\frac{\partial u}{\partial x}+\frac{\partial v}{\partial y}+\frac{\partial w}{\partial z}=0 \tag{1}$$

Momentum Equations

$$\frac{\partial u}{\partial t}+\frac{\partial (uu)}{\partial x}+\frac{\partial (vu)}{\partial y}+\frac{\partial (wu)}{\partial z} = \frac{\partial}{\partial x}\left[(v+vT)\frac{\partial u}{\partial x}\right]+\frac{\partial}{\partial y}\left[(v+vT)\frac{\partial u}{\partial y}\right]+\frac{\partial}{\partial z}\left[(v+vT)\frac{\partial u}{\partial z}\right] + \left(S_u=-\frac{1}{\rho}\frac{\partial p}{\partial x}+S'_u\right) \quad (2) \tag{2}$$

$$\frac{\partial v}{\partial t}+\frac{\partial (uv)}{\partial x}+\frac{\partial (vv)}{\partial y}+\frac{\partial (wv)}{\partial z} = \frac{\partial}{\partial x}\left[(v+vT)\frac{\partial v}{\partial x}\right]+\frac{\partial}{\partial y}\left[(v+vT)\frac{\partial v}{\partial y}\right]+\frac{\partial}{\partial z}\left[(v+vT)\frac{\partial v}{\partial z}\right] + \left(S_v=-\frac{1}{\rho}\frac{\partial p}{\partial x}+S'_v\right) \quad (3) \tag{3}$$

$$\frac{\partial w}{\partial t}+\frac{\partial (uw)}{\partial x}+\frac{\partial (vw)}{\partial y}+\frac{\partial (ww)}{\partial z} = \frac{\partial}{\partial x}\left[(v+vT)\frac{\partial w}{\partial x}\right]+\frac{\partial}{\partial y}\left[(v+vT)\frac{\partial w}{\partial y}\right]+\frac{\partial}{\partial z}\left[(v+vT)\frac{\partial w}{\partial z}\right] + \left(S_w=-\frac{1}{\rho}\frac{\partial p}{\partial x}+S'_w\right) \quad (4) \tag{4}$$

Navier Stokes Equations

The law of conservation of momentum for viscous flow is expressed by Navier Stokes equations, which take the following form for incompressible flow and constant property flow and with no body forces in x, y and z directions respectively.

$$\frac{\partial u}{\partial t}+(\mathbf{u}.\nabla)u=-\frac{1}{\rho}\frac{\partial p}{\partial x}+v\nabla^2 u \tag{5}$$

$$\frac{\partial v}{\partial t}+(\mathbf{u}.\nabla)v=-\frac{1}{\rho}\frac{\partial p}{\partial x}+v\nabla^2 v \tag{6}$$

$$\frac{\partial w}{\partial t} + (\mathbf{u}.\nabla)w = -\frac{1}{\rho}\frac{\partial p}{\partial x} + \nu\nabla^2 w \tag{7}$$

where

$$u.\nabla = u\frac{\partial}{\partial x} + v\frac{\partial}{\partial y} + w\frac{\partial}{\partial z}$$

$$\nabla^2 = \frac{\partial^2}{\partial x^2} + \frac{\partial^2}{\partial y^2} + \frac{\partial^2}{\partial z^2}$$

Energy Equation

$$\frac{\partial}{\partial t}(\rho E) + \frac{\partial}{\partial x_i}[u_i(\rho E + P)] = \frac{\partial}{\partial x_j}\left[k\frac{\partial T}{\partial x_j}u_i(\tau_{ij})\right] + S_h \tag{8}$$

Where E is the total energy, k is the thermal conductivity, and (τ_{ij}) is represents viscous heating and defined as follows:

$$(\tau_{ij}) = \mu\left(\frac{\partial u_j}{\partial x_i} + \frac{\partial u_i}{\partial x_j}\right) - \frac{2}{3}\mu\frac{\partial u_i}{\partial xi}\delta_{ij} \tag{9}$$

Where δ_{ij} is Kroneker delta which is 1 for i=j and 0 for i ≠ j.

Wherei or j=1 for x direction

i or j=2 for y direction

i or j=3 for z direction

and

x_1=x,x_2=y, x_3=z

as per the coordinate system (Figure 1) adopted.

The above equations (5) to (7) and (8), (9) are simplified. As the flow involved for the present investigation is turbulent, the modification in these equations for analyzing turbulent flow are incorporated after discussing various simplification, like Reynolds Averaging approach & Boussinesq Approach for the present studies are discussed(5) to (9) equations.

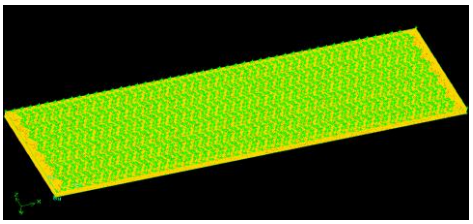

Figure 1: Meshing of the Multi V-Shaped Ribs with Gap Roughened Solar Air Heater Duct

Modeling in GAMBIT

Analysis the problem with CFD the geometry of the flow domain of the solar air heater has been prepared. The arrangement of roughness elements in the form of multi V-shaped ribs with gap fixed on the underside of the absorber plate has been considered. The solution domain used for CFD analysis has been generated as shown in Figure 2.

The GAMBIT 2.3.16 is used for modeling the flow domain with relative width ratio (W/w) of 6, relative gap distance (Gd/Lv) of 0.8, relative roughness pitch (P/e) of 10, relative roughness height (e/D) of 0.043, angle of attack (α) of 30°, relative gap width (g/e) of 1.0.The duct used for CFD analysis having the height (H) of 25 mm and width (W) of 300 mm. The 3D solution domain and grid were selected is shown in Figure 2. There was a need to place very fine mesh near the ribs to predict the results accurately. The total number of nodes in those domains is more than 500,000 and total number of tetrahedrons is more than 1,400,000.

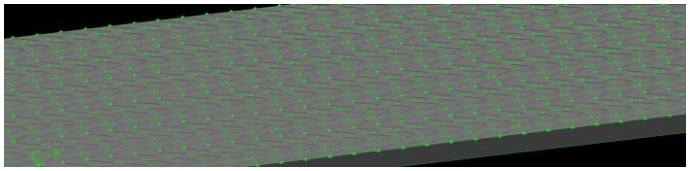

Figure 2: Domain Solution for CFD Analysis Multi V-Shaped Ribs with Gap Roughened Solar Air Heater Duct

Analysis in FLUENT

The different boundary conditions for the geometries are selected air inlet velocity, outlet pressure. In the present numerical model, a uniform heat flux is specified on the top wall (heated wall) which defined at the same value of the experimental conditions and other faces is considered adiabatic asshown in the Figure 3.

Selection and Validation of Model

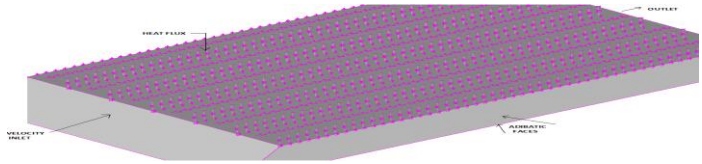

Figure 3: Boundary Conditions

The selection of model is carried out by comparing the predictions by different models namely Standard k-epsilon model, Realizable k-epsilon model, Renormalization k-epsilon model and Shear Stress Transport (SST) k-omega models with experimental results.

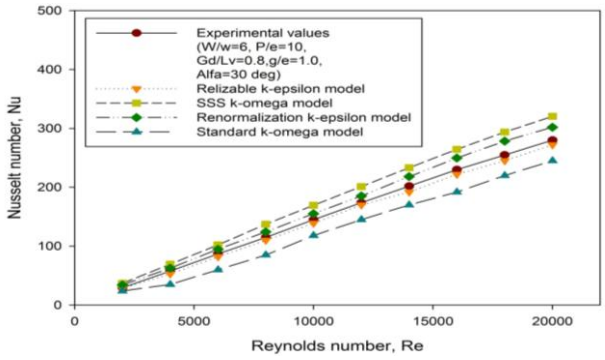

Figure 4: Comparison between Nusselt Number Predictions of Different CFD Models with Experimental Results for Multi -V Shaped Ribs with Gap

Figure 4 shows the variation of Nusselt number with Reynolds number for different models and the experimental results computed from multi V-shaped ribs with gap(W/w=6,P/e=10,e/D=0.043,Gd/Lv=0.8,g/e=1.0,α=30°). It has been observed that the results obtained by Realizable k-epsilon model are in good agreement with multi V-shaped ribs with gap. It is therefore, for the present numerical study Realizable k-epsilon model has been employed to simulate the flow and heat transfer.

Realizable K-Epsilon Model

The Realizable approach which is a mathematical technique, that can be used to derive a turbulence model similar to the k-ε results in a modified form of the epsilon equation which attempts to account for the different scales of motion through changes to the production term.

In the case of turbulent flow, the random nature of flow precludes computational based on a complete description of the motion of all fluid particles. In the present study, the k-epsilon turbulent model with enhanced wall functions for the near wall treatment were used to model for turbulent flow regime. The following equations were used for this purpose.

RESULTS AND DISCUSSIONS

Temperature Profile

The atmospheric air enters at the rectangular duct along x-axis. The upper side of the duct is considered hot absorber plate and uniform distribution of heat flux. In the turbulent region the velocity of the particles very near to surface almost zero. In this region the particles have low kinetic energy. This region is laminar sub layerthis laminar layer act as a barrier of heat transfer to fluid medium as shown in the Figure 5.

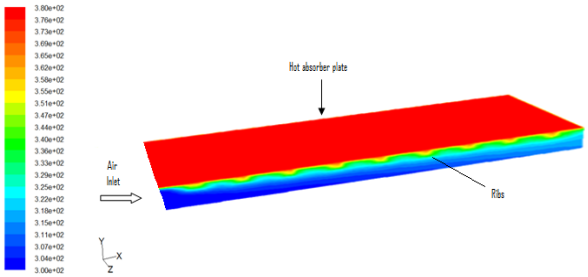

Figure 5: Temperature Profile in the Multi V-Shaped Ribs with Gap Roughened Solar Air Heater Duct

Velocity Profile

Shaping of a long ,angled rib into V-shape ribs help in the formation of two leading ends(where heat transfer rate is high) and a single trailing ends(where heat transfer rate is low) resulting in much large increase of heat transfer. As shown in Figure 6 increasing the relative gap width ratio (W/w) also increasing leading ends and number of secondary flow cells.

Multi v-shaped rib with gap are attached underside of the absorber plate and these ribs breaking and disturbing laminar sub layers and results the temperature of air close to surface is higher, and goes on decreasing away from the surface up to one third height of the duct. The maximum temperature is indicating by the red color and lowest temperature indicates by the blue color.

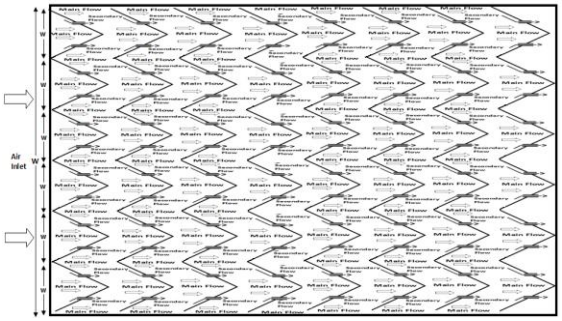

Figure 6: Secondary Flow Pattern for Creating Gap in Multi V-Shaped Ribs

Producing gap in the Multi v-shaped ribs allow releasing secondary flow as shown in Figure 7 (a) & (b) in the present Computational fluid dynamics (CFD) based analysis Multi v-shaped ribs with gap considered underside of the absorber plate. The atmospheric air enter at the rectangular duct and flows under absorber plate which is uniform distribution ofheat flux as seen in the Figure 7and the inlet of the duct air temperature is minimum (indicate blue color is minimum temperature).

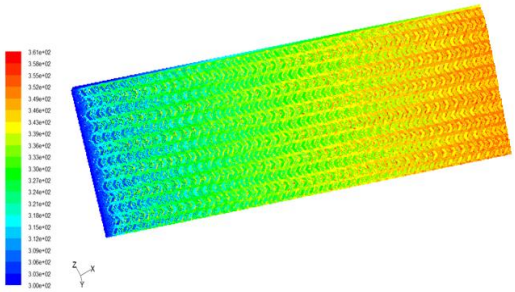

Figure 7(a): Velocity Profile on the Multi V-Shaped Ribs with Gap Roughened Solar Air Heater Duct at Reynolds Number of 2,000

Creating gap in the Multi v-shaped ribs allow release of the secondary flow along the rib joins the main flow to accelerate it, which energizes the retarded boundary layer flow along surface resulting in enhancement of heat transfer as shown in Figure 7(a & b) the air temperature increase (indicate red color is maximum temperature) along the length of the duct.

The comparison Nusselt number and friction factor between the experimental results [9] and CFD results with Realizable k-epsilon model for Multi v-shaped ribs with gap (W/w=6,P/e=10,g/e=1.0,e/D=0.043,Gd/Lv=0.8,α=30°) and as well as the prediction error as given in the Tables. 1 and 2.

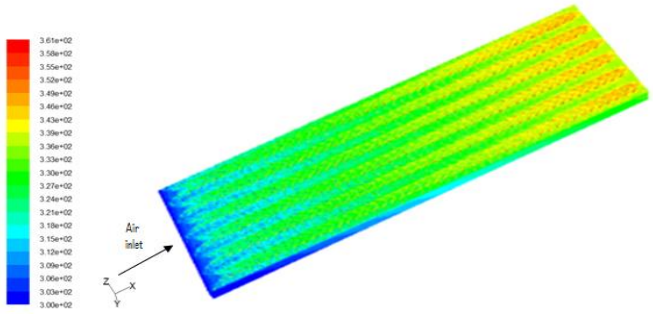

Figure 7(b): Velocity Profile on the Multi V-Shaped Ribs with Gap Roughened Solar Air Heater Duct at Reynolds Number of 20,000

Table 1 The comparison Nusselt number between the experimental results (Ref.9) and CFD results (Realizabke k-epsilon model) for Multi v-shaped ribs with gap (W/w=6,P/e=10,g/e=1.0,e/D=0.043,Gd/Lv=0.8,α=30°) and as well as the prediction error.

Table 1

Sr. No	Reynolds Number (Re)	Velocity (M/S)	Experimental Results [9]	CFD Results	Error (%)
1.	2000.97	0.7404	30.54	31.12	1.899
2.	3999.12	1.4798	63.23	65.07	2.91
3.	6005.02	2.2200	93.78	96.89	3.316
4.	7997.98	2.9595	126.44	130.76	3.417

Table 1: Contd.,					
5.	9999.46	3.7001	156.28	161.84	3.558
6.	12007.10	4.4430	185.61	193.26	4.122
7.	14010.45	5.1843	212.17	221.69	4.487
8.	16025.69	5.9316	237.94	248.86	4.589
9.	18000.21	6.660	263.23	275.44	4.639
10.	20000.11	7.4006	285.33	299.16	4.847

Table 2 The comparison Friction factor between the experimental results (Ref.9) and CFD results (Realizable k-epsilon model) for Multi v-shaped ribs with gap (W/w=6,P/e=10,g/e=1.0,e/D=0.043,Gd/Lv=0.8,α=30°) and as well as the prediction error.

Table 2

Sr. No	Reynolds Number (Re)	Velocity (M/S)	Experimental Results [9]	CFD Results	Error (%)
1.	2000.97	0.7404	0.05111	0.05153	0.822
2.	3999.12	1.4798	0.04468	0.04538	1.567
3.	6005.02	2.2200	0.04124	0.04211	2.109
4.	7997.98	2.9595	0.03775	0.03865	2.384
5.	9999.46	3.7001	0.03443	0.03554	3.224
6.	12007.10	4.4430	0.03157	0.03273	3.674
7.	14010.45	5.1843	0.02979	0.031109	4.428
8.	16025.69	5.9316	0.02766	0.02895	4.664
9.	18000.21	6.6600	0.02568	0.02699	5.101
10.	20000.11	7.4006	0.024567	0.02585	5.222

CONCLUSIONS

Based on CFD based study on angle of attack(α) 30° multi V-shaped ribs with gap roughened solar air heater duct, the following conclusions can be drawn.

- Creating gap in the multi V-shaped ribs arrangement enhance the heat transfer and friction factor of the roughened solar air heater duct. The increase in Nusselt number is in the range of 4 to 5 times of the smooth solar air heater duct.
- The maximum values of Nusselt number and friction factor are observed for a gap in the multi V-shaped ribs with a relative gap width(g/e) of 1.0.
- Computational Fluid Dynamics (CFD) methods are used in the present work for analyzing the gap in the multi V-shaped ribs roughness under consideration. The CFD Realizable k-epsilon model results give the good agreements with experimental results. Hence, CFD techniques can be use for analyzing the temperature profile and velocity profile in the roughness surface.

REFERENCES

1. Momin, A-M E. Saini, J.S. and Solanki, S.C., (2002).Heat transfer and friction in solar air heater duct with V-shaped rib roughness on absorber plate, Int.Journal of Heat and Mass Transfer, 45, pp. 3383 –3396.
2. Momin, A-M E. Saini, J.S. and Solanki, S.C., (2002).Heat transfer and friction in solar air heater duct with V-shaped rib roughness on absorber plate, Int. Journal of Heat and Mass Transfer, 45, pp. 3383 –3396.

3. Karwa, R., (2003). Experimental studies of augmented heat transfer and friction in asymmetrically heatedrectangular ducts with ribs on the heated wall in transverse, inclined, V-continuous and V-discrete pattern, Int. Comm. Heat Mass Transfer, 30, pp. 241 – 250.

4. Sahu, M.M. and Bhagoria, J.L., (2005). Augmentation ofheat transfer co-efficient by using 90° broken transverserib on absorber plate of solar air heater, Renewable Energy, 30, pp. 2057 – 2073.

5. Aharwal, K.R. Gandhi, B.K. and Saini, J.S., (2006).Effect of gap in inclined ribs on the performance ofartificially roughened solar air heater duct, Advancesin Energy Research, pp.144-150.

6. Aharwal, K.R. Gandhi, B.K. and Saini, J.S., (2008).Experimental investigation on heat transfer enhancement due to a gap in an inclined continuous ribarrangement in a rectangular duct of solar air heater,Renewable energy, 33, pp. 585 – 596.

7. Saini, R.P. &Verma, J., (2008). Heat transfer and frictioncorrelations for a duct having dimple shape artificial roughness for solar air heater, Energy, 33, pp. 1277-1287.

8. Bopche S.B. and Tandale M.S., (2009). Experimentalinvestigation on heat transfer and friction characteristics of a turbulator roughened solar air heater duct, International Journal of heat and Mass Transfer, 52, pp. 2834 – 2848.

9. Anil Kumar, R. P. Saini, J.S. Saini. Development of correlations for Nusselt number and friction factor for solar air heater with roughened duct having multi v-shaped with gap rib as artificial roughness.Renewable Energy, Volume 58, October 2013, Pages 151-163